3

Photoluminescence in Low-dimensional Oxide Ferroelectric Materials

Dinghua Bao
State Key Laboratory of Optoelectronic Materials and Technologies, School of Physics and Engineering, Sun Yat-Sen University, Guangzhou, 510275 P.R. China

1. Introduction

Ferroelectric materials exhibit important multifunctional electrical properties such as ferroelectric, dielectric, piezoelectric, pyroelectric, and electrooptic properties. They can be used to fabricate various microelectronic and optoelectric devices including nonvolatile ferroelectric random access memories, microsensors and microactuators, integrated capacitors, and electrooptic modulators [1-3]. Widely studied ferroelectric materials include $Pb(Zr,Ti)O_3$ (PZT), lanthanide doped $Bi_4Ti_3O_{12}$ (BiT), and $BaTiO_3$.

PZT is the most important piezoelectric material which has been used in various electronic devices. $BaTiO_3$ and its solid solution with $SrTiO_3$ exhibit high dielectric constant and other advantageous properties. Lanthanide doped BiT gained great interest on searching new ferroelectric thin films with fatigue-free polarization properties for non-volatile random access memories. Among them, La doped bismuth titanate and Nd-doped bismuth titanate exhibit excellent electrical properties such as high fatigue resistance, good retention, fast switching speed, high Curie temperature, large spontaneous polarization, and small coercive field [2-4]. In addition, lanthanide doped BiT do not contain lead, thus, environmental pollution and harm to health of human due to lead volatility in PZT can be avoided. Studies in the past decade indicate that lanthanide doped bismuth titanate ferroelectric thin films are the most promising candidate materials for nonvolatile ferroelectric random access memory applications. Most efforts have been devoted to improving the electrical properties of $Bi_4Ti_3O_{12}$ (BIT) thin films by rare earth ion doping for the development of non-volatile ferroelectric random access memory applications [5-7]. It is worth pointing out that besides excellent ferroelectric polarization fatigue-free characteristics, the bismuth layered perovskite structure ferroelectric thin films also exhibit good piezoelectric properties and large optical nonlinearity [8-10].

Recently, photoluminescence (PL) properties originated from defects or rare earth ions in oxide ferroelectric materials have attracted much attention for possible integrated photoluminescent ferroelectric device applications. This paper briefly reviews the status and new progress on study of photoluminescence in low-dimensional oxide ferroelectric materials including ferroelectric thin films, nanopowders, nanorods or nanowires, and nanotubes, and some of our own research work in this field with an emphasis on the photoluminescence properties of lanthanide doped bismuth titanate thin films such as $(Bi,Pr)_4Ti_3O_{12}$, $(Bi,Eu)_4Ti_3O_{12}$, $(Bi,Er)_4Ti_3O_{12}$, and codoped bismuth titanate thin films will be presented in this paper, also.

2. Photoluminescence in ferroelectric nanopowders and nanowires

2.1 Photoluminescence in ferroelectric nanopowders

Photoluminescence from rare earth ions in ferroelectric nanopowders has been studied by some research groups. Badr, et al. studied the effect of Eu^{3+} contents on the photoluminescence of nanocrystalline $BaTiO_3$ powders [11]. The powders were prepared by sol-gel technique using $Ba(Ac)_2$, and $Ti(C_4H_9O)_4$ as raw materials, annealed at 750 ^oC in air for 0.5 h. The crystallite size of the doped sample with 4% Eu^{3+} ions in the powder was found to be equal to 32 nm. The photoluminescence of nanocrystalline powders at 488 nm were observed. The luminescence spectra of ultra fine Eu^{3+}:$BaTiO_3$ powders are dominated by the $^5D_0 \rightarrow {}^7F_J$ (J=0-4) transitions, indicating a strong distortion of the Eu^{3+} sites. The structure disorder and charge compensation were suggested to be responsible for the strong inhomogeneous broadening of the $^5D_0 \rightarrow 7F$ luminescence band of the Eu^{3+}.

Fu, et al. studied characterization and luminescent properties of nanocrystalline Pr^{3+}-doped $BaTiO_3$ powders synthesized by a solvothermal method using barium acetylacetonate hydrate, titanium (IV) butoxide, and praseodymium acetylacetonate hydrate as precursors [12]. They discussed the luminescence mechanism, the band gap change and the size dependence of their fluorescence properties of the powders.

Lemos and coworkers studied up-conversion luminescence properties in Er^{3+}/Yb^{3+}-codoped $PbTiO_3$ perovskite powders prepared by Pechini method [13]. Efficient infrared-to-visible conversion results in green (about 555 nm) and red (about 655 nm) emissions under 980 nm laser diode excitation. The main up-conversion mechanism is due to the energy transfer among Yb and Er ions in excited states.

On the other hand, photoluminescence from defects such as oxygen vacancies or structure disorder is worth studying. Lin, et al. prepared nanosized $Na_{0.5}Bi_{0.5}TiO_3$ powders with particle size of about 45-85 nm using a sol-gel method and studied their photoluminescence properties [14]. It was observed from photoluminescence spectra that the main emission peak of the nanosized powder exhibited a blue shift from 440.2 to 445.3 nm with decreasing particle size, while the emission intensity increased. They explained that the visible emission band is due to self-trapped excitation, and this blue shift of the main emission was attributed to distortion of TiO_6 octahedra originated from the surface stress of $Na_{0.5}Bi_{0.5}TiO_3$ crystallite and the dielectric confinement effect.

Oliveira and coworkers studied synthesis and photoluminescence behavior of $Bi_4Ti_3O_{12}$ (BiT) powders obtained by the complex polymerization method [15]. The BiT powders annealed at 700 ^oC for 2 h under oxygen flow show an orthorhombic structure without impurity phases. UV-vis spectra indicated that there are intermediary energy levels within the band gap of the powders annealed at low temperatures. The maximum PL emissions were observed at about 598 nm, when excited by 488 nm wavelengths. Also, it was observed that there were two broad PL bands, which were attributed to the intermediary energy levels arising from alpha-Bi_2O_3 and BiT phases.

Pizani, et al. reported intense photoluminescence observed at room temperature in highly disordered (amorphous) $BaTiO_3$, $PbTiO_3$, and $SrTiO_3$ prepared by the polymeric precursor method [16]. The emission band maxima from the three materials are in the visible region and depend on the exciting wavelength. The authors thought that photoluminescence could be related to the disordered perovskite structure.

Highly intense violet-blue photoluminescence at room temperature was also observed with a 350.7 nm excitation line in structurally disordered $SrZrO_3$ powders by Longo, et al [17].

They discuss the role of structural order-disorder that favors the self-trapping of electrons and charge transference, as well as a model to elucidate the mechanism that triggers photoluminescence. In this model the wide band model, the most important events occur before excitation.

They also reported room temperature photoluminescence of $Ba_{0.8}Ca_{0.2}TiO_3$ powders prepared by complex polymerization method [18]. Inherent defects, linked to structural disorder, facilitate the photoluminescence emission. The photoluminescent emission peak maximum was around of 533 nm (2.33 eV) for the $Ba_{0.8}Ca_{0.2}TiO_3$. The photoluminescence process and the band emission energy photon showed dependence of both the structural order-disorder and the thermal treatment history.

Intense and broad photoluminescence (PL) emission at room temperature was observed on structurally disordered $Ba(Zr_{0.25}Ti_{0.75})O_3$ (BZT) and $Ca(Zr_{0.05}Ti_{0.95})O_3$ (CZT) powders synthesized by the polymeric precursor method [19,20]. The theoretical calculations and experimental measurements of ultraviolet-visible absorption spectroscopy indicate that the presence of intermediary energy levels in the band gap is favorable for the intense and broad PL emission at room temperature in disordered BZT and CZT powders. The PL behavior is probably due the existence of a charge gradient on the disordered structure, denoted by means of a charge transfer process from $[TiO_5]$-$[ZrO_6]$ or $[TiO_6]$-$[ZrO_5]$ clusters to $[TiO_6]$-$[ZrO_6]$ clusters.

Similar photoluminescence behavior was also observed in disordered $MgTiO_3$ and Mn-doped $BaTiO_3$ powders [21,22]. The experimental and theoretical results indicated that PL is related with the degree of disorder in the powders and also suggests the presence of localized states in the disordered structure.

Blue-green and red photoluminescence (PL) emission in structurally disordered $CaTiO_3$:Sm powders was observed at room temperature with laser excitation at 350.7 nm [23]. The generation of the broad PL band is related to order-disorder degree in the perovskitelike structure.

The photoluminescence from $SrZrO_3$ and $SrTiO_3$ crystalline, quasi-crystalline, and quasi-amorphous samples, prepared by the polymeric precursor method, was examined by ab initio quantum mechanical calculations [24]. It was used in the modeling the structural model consisting of one pyramidal TiO_5 or ZrO_5 unit piled upon the TiO_6 or ZrO_6, which are representative of disordered structures of quasi-crystalline structures such as ST and SZ. In quasi-crystalline powders, the photoluminescence in the visible region showed different peak positions and intensities in SZ and ST. The PL emission was linked to distinct distortions in perovskite lattices and the emission of two colors-violet-blue in SZ and green in ST-was also examined in the light of favorable structural and electronic conditions. First principles calculations on the origin of violet-blue and green light photoluminescence emission in $SrZrO_3$ and $SrTiO_3$ perovskites

Ma, et al. studied synthesis and luminescence of undoped and Eu^{3+}-activated Aurivillius-type Bi_3TiNbO_9 (BTNO) nanophosphors by sol-gel combustion method [25]. Photoluminescence measurements indicated that a broad blue emission was detected for BTNO nanoparticles, and the characteristic Eu^{3+} ions $^5D_0 \rightarrow {}^7F_J$ (J=1-4) transitions were observed for the doped samples. Further investigation illuminates that the Eu^{3+} ions substituted for Bi^{3+} ions at A site in the pseudo-perovskite layers. It can be confirmed from high bright fluorescence image and short decay time that the novel orange-red phosphor has the potential applications in luminescence devices.

2.2 Photoluminescence in ferroelectric nanowires, nanotubes, and nanosheets

Gu, et al. reported characterization of single-crystalline lead titanate nanowires using photoluminescence spectroscopy, and ultraviolet-visible spectroscopy [26,27]. The nanowires were synthesized by surfactant-free hydrothermal method at 200 ^{o}C. The nanowires with uniform diameters of about 12 nm and lengths up to 5 um, exhibit a tetragonal perovskite structure without impurity phases. A blue emission centered at about 471 nm (2.63 eV) is observed at room temperature. Oxygen vacancies are believed to be responsible for the luminescence in the $PbTiO_3$ nanowires.

Chen, et al. prepared ferroelectric $PbHPO_4$ nanowires by a hydrothermal method at 180 °C for 24 h using a single-source precursor, Pb(II)−IP6 (IP6, inositol hexakisphosphate acid) complex [28]. PL measurements indicate that the nanowires exhibit a broad emission peak at 460 nm under the excitation of 375 nm.

Yang et al. reported synthesis of high-aspect-ratio $PbTiO_3$ nanotube arrays by the hydrothermal method [29]. The $PbTiO_3$ nanotube arrays have a tetragonal perovskite structure without any other impurity phases. A strong green emission band centered at 550 nm (2.25 eV) was observed in $PbTiO_3$ nanotube arrays at room temperature. Local defects in $PbTiO_3$ nanotube arrays were thought to result in the photoluminescence behavior.

$PbTiO_3$ nanotube arrays have also been synthesized via sol–gel template method. These nanotubes have a diameter about 300 nm and a length 50 um, with a wall thickness of typically several tens of nanometers. The as-prepared PTO nanotubes possess polycrystalline perovskite structure. An intense and wide emission band centered at 505 nm was observed [30]. The photoluminescence of PTO nanotubes was attributed to the radiative recombination between trapped electrons and trapped holes in localized tail states due to structural disorder and gap states due to a large amount of surface defects and oxygen vacancies.

Ida, et al. successfully prepared layered perovskite $SrBi_2Ta_2O_9$ nanosheets with a thickness of about 1.3 nm. The nanosheets showed visible blue luminescence under excitation at 285 nm at room temperature [31]. The luminescence property of the nanosheets was found to be largely sensitive to the change in the surface environment such as adsorption of H+ and/or OH-.

3. Photoluminescence properties of (Bi, Ln)$_4$Ti$_3$O$_{12}$ thin films

As is known, lanthanide doped bismuth titanate thin films are the most promising candidate materials for ferroelectric nonvolatile random access memory applications due to their superior properties such as nonvolatility, long retention time, high fatigue resistance. Recently, photoluminescence properties originated from some rare earth ions in these kinds of the thin film materials have attracted much attention for possible integrated photoluminescent ferroelectric thin film devices.

3.1 Crystal structure of lanthanide doped bismuth titanate thin films

Lanthanide doped bismuth titanate, $Bi_{4-x}Ln_xTi_3O_{12}$ (BLnT) consists of a layered structure of $(Bi_2O_2)^{2+}$ and $(Bi_2Ti_3O_{10})^{2-}$ pseudo-perovskite layers. Its crystal structure can be formulated as $(Bi_{2-x}Ln_xTi_3O_{10})^{2-}(Bi_2O_2)^{2+}$, in which three perovskite-like unit cells are sandwiched between two bismuth oxide layers along the c axis of the pseudotetragonal structure. The lattice paramenters of $Bi_{4-x}Ln_xTi_3O_{12}$ (using rare element La as an example) are a=0.542 nm,b=0.541 nm, and c=3.289 nm, respectively. The lanthanide ions substitute for the Bi ions

in the pseudo-perovskite layer, and thus enhance the ferroelectric properties. Generally, high fatigue resistance of $Bi_{4-x}Ln_xTi_3O_{12}$ is attributed to the existence of net charge of $(Bi_2O_2)^{2+}$ layer which can compensate for the space charge in the ferroelectric/electrode interface [2]. In addition, good chemical stability of perovskite-like layer makes oxygen vacancies difficultly generate, also contributing the good polarization fatigue-free properties [32]. Due to the layered perovskite structure, $Bi_{4-x}Ln_xTi_3O_{12}$ exhibits strong anisotropic electrical properties, because the vector of the spontaneous polarization in the layered perovskite materials is almost along a axis. Therefore, the anisotropic electrical properties of $Bi_{4-x}Ln_xTi_3O_{12}$ have been widely studied [33-35]. On the other hand, BLnT thin films also show excellent optical properties. For example, $Bi_{3.25}La_{0.75}Ti_3O_{12}$ thin films exhibited remarkable optical nonlinearity [10], and $(Bi, Eu)_4Ti_3O_{12}$ thin films showed red photoluminescence (PL) properties of Eu^{3+} ions [36,37]. The photoluminescence properties of BLnT thin films might have potential applications for integrated photoluminescent ferroelectric thin film devices.

As mentioned before, some of BLnT thin films, e.g. $(Bi,Nd)_4Ti_3O_{12}$, have also been reported to exhibit excellent optical properties such as large optical nonlinearity, high optical transparency in the visible wavelength region, which are attractive for the potential uses in optic and optoelectronic devices. Some rare earth elements such as Eu, Pr, Er in BLnT thin films can, on the one hand, act as a structural modifier which greatly improves the electrical properties of BLnT thin films, on the other hand, these rare earth elements can also act as the activator ions of luminescent materials [36,37]. Besides, $Bi_4Ti_3O_{12}$ (BIT) thin films have a high Curie temperature of 675 ^oC and good chemical stability. In addition, the rare earth ions substitute for the Bi^{3+} sites in perovskite-like layer $(Bi_2Ti_3O_{10})^{2-}$ of BIT, therefore the doping content of the rare earth ions could be large, and no charge compensation is needed. Recent research indicates that these Eu, Pr, Er doped bismuth titanate thin films will possibly be potential luminescent ferroelectric materials.

3.2 $(Bi, Eu)_4Ti_3O_{12}$ luminescent ferroelectric thin films

Ruan, et al. first prepared europium-doped bismuth titanate, $(Bi_{4-x}Eu_x)Ti_3O_{12}$ (BEuT) thin films on indium-tin-oxide (ITO)-coated glass substrates, and studied their photoluminescent properties as well as ferroelectric properties [36,37]. The BEuT thin films prepared by chemical solution deposition had a polycrystalline bismuth-layered perovskite structure. Excellent optical transmittance of the BEuT thin films was confirmed as shown in Fig. 1 [36]. Figure 2 shows emission and excitation spectra of BEuT (x=0.85) thin films annealed at different temperatures [36]. The excitation spectra were monitored at 617 nm and the emission spectra were observed by excitation at 350 nm. Photoluminescence spectra of the thin films included two strong peaks which originated from two transitions of $^5D_0 \rightarrow {}^7F_1$ (594 nm) and $^5D_0 \rightarrow {}^7F_2$ (617 nm) of levels of Eu^{3+} ions [38,39]. The emission peak intensities of the two transitions increase with increasing annealing temperature, due to improved crystallinity of the thin films, resulting in higher oscillating strengths for optical transitions [40,41]. At higher temperature, Eu^{3+} ions can arrive at real lattice sites more easily, thus this leads to enhanced activation of Eu^{3+} ions [42]. Investigation to the effect of Eu^{3+} concentrations (x=0.25, 0.40, 0.55, 0.70, and 0.85, respectively) on the photoluminescence properties of BEuT thin films indicates that there is an unusual composition quenching effect of photoluminescence as shown in Fig.3 [36]. The quenching concentration of BEuT thin films is about 0.40. Similar unusual concentration quenching effect of

photoluminescence has also been observed in some Eu^{3+}-ion-activated layered perovskite luminescent powder materials such as $Na_2Gd_{2(1-x)}Eu_{2x}Ti_3O_{10}$, $NaGd_{1-x}Eu_xTiO_4$, and $RbLa_{1-x}Eu_xTa_2O_7$ [43,44]. It was suggested that in these layered perovskite luminescent powder materials, the energy transfer was restricted in the Eu^{3+} sublattices. Similarly, in our case, BEuT has a bismuth layer perovskite structure, and the Eu^{3+} ions in BEuT thin films are mainly substituting for the Bi^{3+} ions in $(Bi_{2-x}Eu_xTi_3O_{10})^{2-}$ perovskite-like layers rather than in $(Bi_2O_2)^{2+}$ layers, therefore, the energy transfer might occur in the nearby Eu^{3+} ions in the perovskite-like layers, thus resulting in the unusual concentration quenching of BEuT thin films. When the concentration of Eu^{3+} ions exceeds the critical value, the radiative centers increase with increasing doping amount of Eu^{3+} ions, however, at the same time the quenching centers also increase, this would lead to increase of the non-radiative rate, consequently, the PL intensity decreases.

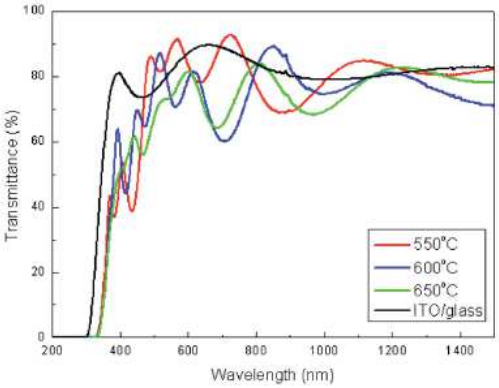

Fig. 1. Optic transmittance of BEuT (x=0.85) thin films annealed at different temperatures. From Ref. [36] Ruan, K.B., et al., *J. Appl. Phys., 103,* 074101 (2008). Copyright American Institute of Physics (2008)

Electrical measurements indicated that the BEuT thin films also showed ferroelectric properties comparable to those of BEuT thin films deposited on $Pt/Ti/SiO_2/Si$ substrates annealed at the same temperature for 1 h [45]. High fatigue resistance was also observed after 10^{10} switching cycles.

For most BLnT thin films, the doping amount of rare ions about 0.85 results in better electrical properties of the thin films [4, 46,47]. However, the quenching concentration x of $Bi_{4-x}Eu_xTi_3O_{12}$ thin films is about 0.40, which is much lower than 0.85. In order to obtain the BLnT thin films with both good electrical and photoluminescent properties at the same time, we proposed to prepare Eu- and Gd- codoped bismuth titanate ($Bi_{3.15}Eu_{0.425}Gd_{0.425}Ti_3O_{12}$, BEGT) thin films with both Eu^{3+} and Gd^{3+} doping amounts being 0.425, giving a total doping amount of rare earth ions of 0.85. It was expected that, on the one hand, the BEGT thin films might exhibit good photoluminescent properties since Eu^{3+} doping amount of 0.425 in the thin films is close to the quenching concentration about 0.40 of BEuT thin films, on the other hand, the BEGT thin films might also show good electrical properties comparable to those of BEuT thin films and of BGdT thin films because total doping amount of rare earth ions is maintained to be 0.85 in the thin films. Figure 7 shows the emission

spectra of BEGT and BEuT thin films under 350 nm exciting wavelength [37]. The enhancement of emission intensities for two Eu^{3+} emission transitions of $^5D_0 \rightarrow {}^7F_1$ (594 nm) and $^5D_0 \rightarrow {}^7F_2$ (617 nm) was observed for the BEGT thin films as compared to BEuT thin films. This photoluminescence improvement can be attributed to Eu content of BEGT thin films close to quenching concentration of BEuT thin films and local distortion of crystal field surrounding the Eu^{3+} activator induced by different ionic radii of Eu^{3+} and Gd^{3+} ions. As mentioned before, the critical value of quenching concentration for $Bi_{4-x}Eu_xTi_3O_{12}$ thin films was near x=0.40. In the case of BEGT thin films, Eu^{3+} doping amount of 0.425 is close to the quenching concentration 0.40 of BEuT thin films, therefore, BEGT thin films exhibit better photoluminescence than $Bi_{3.15}Eu_{0.85}Ti_3O_{12}$ thin films. In addition, local distortion of crystal field surrounding the Eu^{3+} activator induced by different ionic radii of Eu^{3+} and Gd^{3+} ions in BEGT thin films also contributes to the enhancement of photoluminescence.

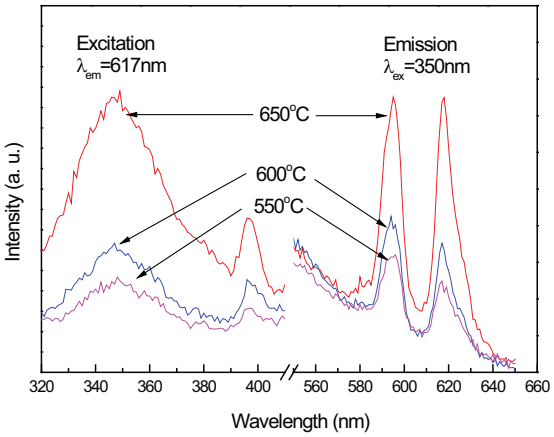

Fig. 2. Excitation and emission spectra of BEuT (x=0.85) thin films annealed at different temperatures. From Ref. [36] Ruan, K.B., et al., J. Appl. Phys., 103, 074101 (2008). Copyright American Institute of Physics (2008)

In addition, the BEGT thin films had larger remanent polarization and higher dielectric constant than BGdT and BEuT thin films prepared under the same experimental conditions. Therefore, co-doping of rare earth ions such as Eu and Gd in bismuth titanate thin films is an effective way to improve photoluminescence and electrical properties of the thin films.

As mentioned before, the bismuth layered perovskite structure BLnT exhibits strong structural anisotropy, which results in strong crystallographic orientation dependence of ferroelectric properties. Many studies indicate that c-axis-oriented (001) epitaxial $(Bi,La)_4Ti_3O_{12}$, $(Bi,Nd)_4Ti_3O_{12}$ thin films exhibit a very low remanent polarization along the film normal, because the vector of the spontaneous polarization in the layered perovskite materials is almost along a axis. Therefore, it is of interest to know whether there is similar orientation dependence of PL properties of BEuT thin films [48].

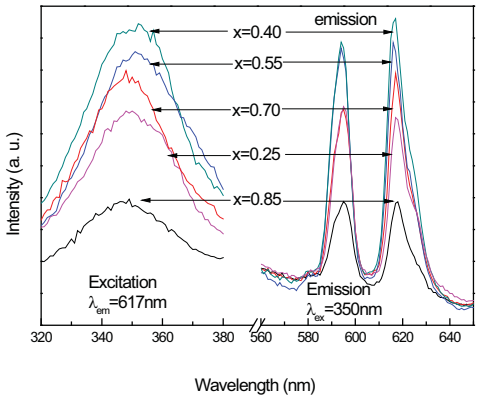

Fig. 3. Photoluminescence spectra of BEuT thin films with different Eu^{3+} concentrations. From Ref. [36] Ruan, K.B., et al., J. Appl. Phys., 103, 074101 (2008). Copyright American Institute of Physics (2008)

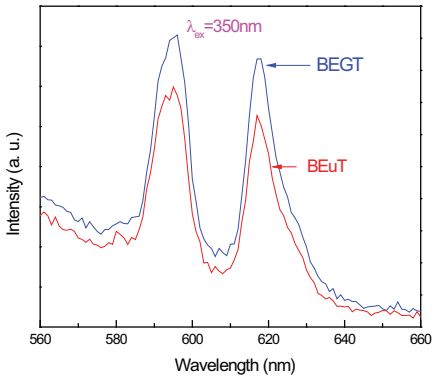

Fig. 4. Emission spectra of BEGT and BEuT thin films under exciting wavelength of 350 nm. From Ref. [37] Ruan, K.B., et al., J. Appl. Phys., 103, 086104 (2008). Copyright American Institute of Physics (2008)

The BEuT thin films were prepared on STO (100) and STO (111) substrates by using chemical solution deposition, and the effects of Eu ion concentration and crystallographic orientation on photoluminescent property of the thin films were investigated. The BEuT thin films prepared on STO (100) substrates grew with high c axis orientation due to very small film/substrate lattice mismatch, whereas BEuT thin films prepared on STO (111) substrates crystallized with random orientation. Figure 5 shows the PL emission spectra of $Bi_{4-x}Eu_xTi_3O_{12}$ thin films with different Eu ion concentrations on STO (100) substrates [48]. From Fig. 5, it can be observed that the PL intensity is obviously related to the doping amount of Eu^{3+} ions. The maximum PL intensity was obtained for the BEuT thin films with Eu^{3+}

concentration of x=0.55. It is worth noting that the quenching concentration of BEuT thin films prepared on STO (100) substrates is higher than that (x=0.4) for the thin films on ITO-coated glass. This may be ascribed to effects of the crystal orientation of BEuT thin films. The BEuT thin films prepared on STO (100) substrates show high c axis orientation, while BEuT thin films on ITO-coated glass and quartz substrates exhibit random orientation. For randomly oriented thin films, more non-radiative defects existed in the grain boundaries, resulting in decrease of quenching concentration.

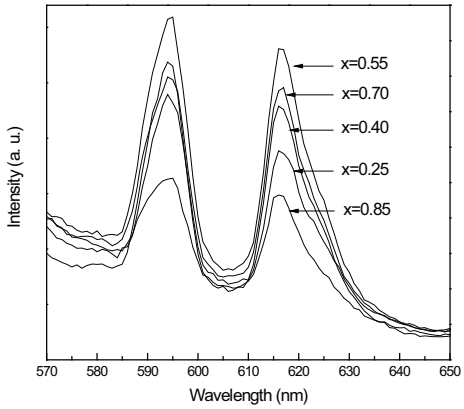

Fig. 5. PL emission spectra of $Bi_{4-x}Eu_xTi_3O_{12}$ thin films on STO (100) substrates (λ_{ex}=350 nm). Ref. [48] Ruan, K.B., et al., J. Appl. Phys., 104, 036101 (2008). Copyright American Institute of Physics (2008)

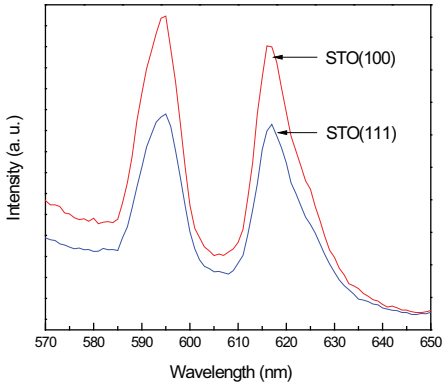

Fig. 6. PL emission spectra of $Bi_{3.45}Eu_{0.55}Ti_3O_{12}$ thin films prepared on STO (100) and STO (111) substrates. Ref. [48] Ruan, K.B., et al., J. Appl. Phys., 104, 036101 (2008). Copyright American Institute of Physics (2008)

Figure 6 shows the PL emission spectra of $Bi_{3.45}Eu_{0.55}Ti_3O_{12}$ thin films prepared on STO (100) and STO (111) substrates [48]. It can be observed that the emission intensity of BEuT thin films on STO (100) substrate is obviously stronger than that on STO (111) substrate. On the one hand, the orientation difference of the thin films might affect PL properties of BEuT thin films, specifically, well-aligned grains with c-axis oriented growth lead to low light scattering; on the other hand, the surface roughness may also affect detection of PL properties of thin film materials. It has been reported that rougher surfaces of photoluminescent thin films reduce internal reflections [49]. However, our AFM observation showed that the root mean square roughness values of both the BEuT thin films on the two different substrates are close (15.2 nm on STO (100) substrate and 13.8 nm on STO (111) substrate, respectively). This implies that different PL properties are mainly caused by the orientation difference of BEuT thin films. Note that different from orientation dependence of ferroelectric properties of the rare earth doped bismuth titanate thin films, the c-axis oriented BEuT thin films on STO (100) substrates exhibited stronger photoluminescence than the randomly oriented thin films on STO (111) substrates.

3.3 Nanocomposite films composed of ferroelectric $Bi_{3.6}Eu_{0.4}Ti_3O_{12}$ matrix and highly c-axis oriented ZnO nanorods

PL properties of BEuT thin films might have potential applications for integrated photoluminescent ferroelectric thin film devices. However, further enhancement of emission intensity of BEuT is desirable. For this purpose, Zhou, et al. developed a hybrid chemical solution method to prepare nanocomposite films composed of ferroelectric BEuT matrix and highly c-axis oriented ZnO nanorods with an attempt to achieve a more efficient energy transfer from ZnO nanorods to Eu^{3+} ions in BEuT, and thus, to enhance the PL intensity of BEuT [50].

Figure 7 shows emission spectra of (a) the nanocomposite film composed of BEuT matrix and highly c-axis oriented ZnO nanorods and (b) the BEuT thin film [50]. The excitation wavelength is chosen as 350 nm, as the internal band excitation is more efficient than the intrinsic excitation of Eu^{3+} in BEuT host. Compared with individual BEuT thin film, the nanocomposite film of BEuT matrix and ZnO nanorods exhibits much more intense emissions centered at 594 nm and 617 nm from Eu^{3+} ions. The emission intensities are about 10 times stronger than those for individual BEuT thin film. At the same time, in the emission spectrum, a sharp UV emission at about 380 nm and a broad band emission centered at 525 nm are also observed. The former can be attributed to near band edge emission of ZnO, and the latter is commonly believed to originate from defect-related deep-level emission in ZnO, such as the radiative recombination of photo-generated holes with electrons occupying the oxygen vacancies.

By comparing the emission spectrum of the nanocomposite film composed of BEuT matrix and highly c-axis oriented ZnO nanorods and excitation spectrum of the BEuT thin film, it was found that there are two spectral overlaps between the emission bands of ZnO nanorods and the absorption bands of Eu^{3+} ions in BEuT. One is located between sharp UV emission at 380 nm of ZnO and transition of $^7F_0 \rightarrow {}^5L_6$ at 395 nm of Eu^{3+} ions, and the other one is between defect-related deep-level emission band centered at 525 nm of ZnO and transition of $^7F_0 \rightarrow {}^5D_2$ at 465 nm of Eu^{3+} ions. It has been believed that energy transfer occurs only when the emission band of sensitizer (ZnO in this study) overlaps spectrally with the absorption band of activator (Eu^{3+} ions in this study). In our case, under the excitation of 350

nm radiation, ZnO nanorods firstly absorb the radiation energy, and promote electrons to move from the valence band to the conduction band, leading to band edge emission of ZnO. Then, due to the spectral overlap between the band edge emission of ZnO nanorods and the $^7F_0 \rightarrow {}^5L_6$ excitation spectrum of Eu^{3+} ions centered at 395 nm in BEuT, an efficient energy transfer from the ZnO nanorods to Eu^{3+} ions occurs, promoting the Eu^{3+} ions from $^7F_0$ ground state to $^5L_6$ excited state [51]. The Eu^{3+} ions in the excited state $^5L_6$ undergo nonradiative decay to the $^5D_0$ state because the gaps of adjacent levels are small. Then, radiative transition takes place between the $^5D_0$ and the ^7F_J (J=0–6) states because of the larger gap [52,53]. This is one of the reasons that red PL of Eu^{3+} ions can be enhanced.

On the other hand, the defect states such as oxygen vacancies in the ZnO nanorods also capture electrons, and generate a broad band green emission centered at 525 nm. Due to the spectral overlap between the defect-related emission of ZnO and the absorption band of $^7F_0 \rightarrow {}^5D_2$ transition at 465 nm of Eu^{3+} ions, an efficient energy transfer also occurs. Thus, some Eu^{3+} ions are promoted from the ground state $^7F_0$ to the excited state $^5D_2$. Similarly, this can also result in enhancement of red PL of Eu^{3+} ions. It has been reported that the defect states (trapping centers) in ZnO can temporarily store the excitation energy, then giving rise to efficient energy transfer from the traps in ZnO to Eu^{3+} ions [53].

For nonradiative energy transfer, the distance between the emission and absorption centers must be very close [51]. Therefore, in Eu^{3+}-doped ZnO materials the energy transfer is nonradiative energy transfer [54,55]. However, in our nanocomposite films, the energy transfer should be a radiative energy transfer because the BEuT matrix can only contact with the outside part of the ZnO nanorods. It has been reported that in some other materials with Eu^{3+} as activators combined with ZnO quantum dots or ZnO thin films the energy transfer is radiative energy transfer [51, 56].

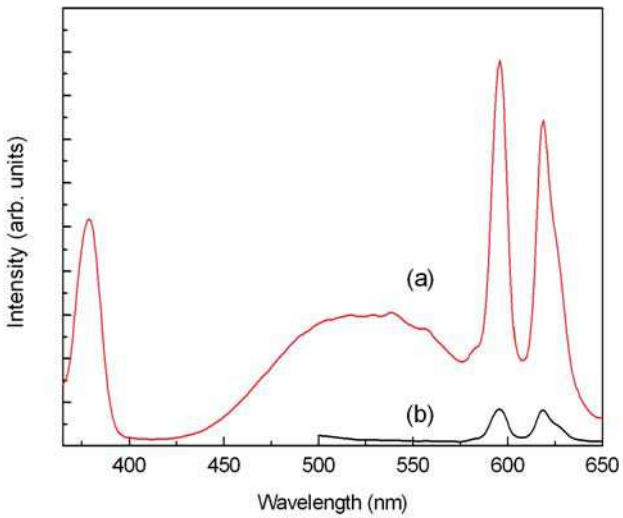

Fig. 7. Emission spectra of (a) the nanocomposite film composed of BEuT matrix and highly c-axis oriented ZnO nanorods and (b) the BEuT thin film. From Ref. [50] Zhou, H., et al., J. Am. Chem. Soc., 132, 1790 (2010). Copyright American Chemical Society (2010)

3.4 $(Bi, Pr)_4Ti_3O_{12}$ luminescent ferroelectric thin films

Recently, Pr doped $ATiO_3$ (A=Sr, Ca) titanate thin films have been widely studied for photoluminescence applications. Usually these thin films exhibit three emission peaks, which are located at 493 nm, 533 nm, and 612 nm, respectively [57]. Of them, the strongest peak is at about 612 nm. It is known that the lattice distortion of host materials and/or site symmetry of rare ions greatly affect the photoluminescence properties. Since Pr doped $SrTiO_3$ or $CaTiO_3$ thin films have simple perovskite structure, whereas Pr^{3+}-doped BIT (BPT) presents bismuth layered perovskite structure, and correspondingly, site symmetry of Pr ions is different, Pr^{3+}-doped BIT thin films are expected to show different photoluminescent properties. Our study confirmed that BPT thin films also exhibit three emission peaks, at 493 nm, 533 nm, and 612 nm, respectively, however, strongest peak is at 493 nm when Pr doping content is large than 0.01. It was observed that the $Bi_{3.91}Pr_{0.09}Ti_3O_{12}$ thin films have highest photoluminescence intensity, in other words, the quenching concentration for 493 nm emission is 0.09. Note that the doping amount of Pr^{3+} ions was so small that the ferroelectric properties of BPT thin films were not good. Taking into consideration that lanthanum doped BIT thin films exhibited good electrical properties, such as relatively high remanent polarization, low processing temperature, and good polarization fatigue-free properties, and that La^{3+} are usually used as host ions in rare earth luminescence materials because La^{3+} ions do not absorb ultraviolet emission, therefore, La^{3+} ions were selected to incorporate into $Bi_{3.91}Pr_{0.09}Ti_3O_{12}$ thin films in order to improve the photoluminescence and electrical properties of the thin films. The results confirmed that both the photoluminescence and ferroelectric polarization of BPT thin films have been enhanced by La^{3+} doping [58].

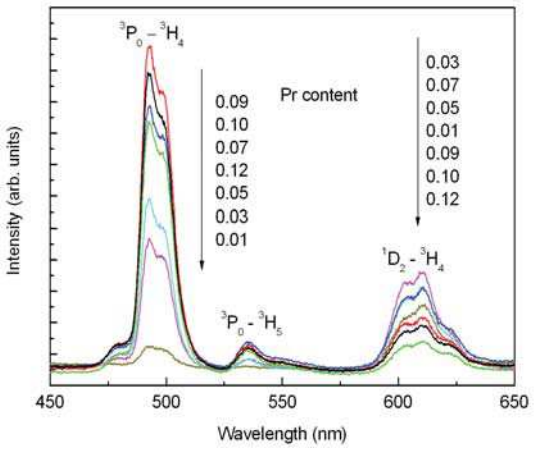

Fig. 8. Photoluminescence spectra of BPT thin films with different Pr contents. From Ref. [58] Zhou, H., et al., J. Am. Ceram. Soc., 93, 2109 (2010) Copyright American Ceramic Society (2010)

Figure 8 shows photoluminescence spectra of BPT thin films with different Pr^{3+} contents [58]. It can be observed that under the 350 nm UV excitation, the emission spectra include three peaks at around 493, 533 and 612 nm, which can be assigned to the transitions of $^3P_0 \rightarrow {}^3H_4$, $^3P_0 \rightarrow {}^3H_5$, and $^1D_2 \rightarrow {}^3H_4$ of Pr^{3+} ions, respectively. As Pr^{3+} ion content increases, the intensities of the blue-green (493 nm) emissions increase first, and then decrease. When Pr^{3+}

ion content is 0.09, the blue-green emission reaches maximum, indicating that the quenching concentration of the blue-green emission is 0.09. We note that the red emission (612 nm) has been relatively weak for all Pr doping contents except Pr doping content of 0.01. This is very different from that of Pr^{3+} doped $SrTiO_3$ and $CaTiO_3$ thin films in which the red emission is strongest whereas the blue-green emission is very weak [59,60]. This is because the photoluminescence properties of Pr^{3+} are sensitive to host lattice symmetry. There is obvious difference of host lattice between Pr doped titanate with simple perovskite structure and BPLT with bismuth layered perovskite structure. It has been reported that, in Pr^{3+} doped $CaSnO_3$ perovskite with an orthorhombic symmetry, the emission from $^3P_0$ to $^3H_4$ (blue-green) is dominant over $^1D_2$ to $^3H_4$ red emission [61]. Okumura and coworkers confirmed that the $^3P_0 \rightarrow {}^3H_4$ transition (blue-green) in $R_2O_3:Pr^{3+}$ (R=Y, La and Gd) became dominant instead of $^1D_2 \rightarrow {}^3H_4$ transition (red) when the crystal structure was distorted from cubic to monoclinic [62]. Besides the difference of their crystal structures, local structure or site symmetry of Pr ions should have a large influence on photoluminescence properties.

As is known, BIT layered perovskite has a monoclinic symmetry below Tc, but it can be represented as orthorhombic with the c-axis perpendicular to the $(Bi_2O_2)^{2+}$ layers. In BIT, a perovskite-like $(Bi_2Ti_3O_{10})^{2-}$ layer consists of three layers of TiO_6 octahedra, where Bi ions occupy the spaces in the framework of TiO_6 octahedra, and rare earth ions only substituted Bi^{3+} ions at $(Bi_2Ti_3O_{10})^{2-}$ perovskite layers. Owing to different lattice structures of BPT from $ATiO_3$ (A=Sr, Ca), BPT exhibits different photoluminescent properties. Since the transition from $^3P_0$ to $^3H_4$ is spin-allowed, it is understandable that the blue-green emission is dominant in the BPT thin films.

In order to improve the photolumincesence and ferroelectric properties, we fixed the Pr content at 0.09, and then added different content La ions into PBT thin films. Figure 9 shows photoluminescence spectra of BPLT-x thin films with various La contents [58]. Under the 350 nm UV excitation, the BPLT-x thin films also exhibit a strong blue-green emission peak at 493 nm, together with the other two weaker emission peaks at 533 nm and 612 nm, respectively. As can be seen, the peaks of emission spectra are similar for all the thin films, but their emission intensities vary with the La content. When La content x is 0.36, the emission reaches maximum.

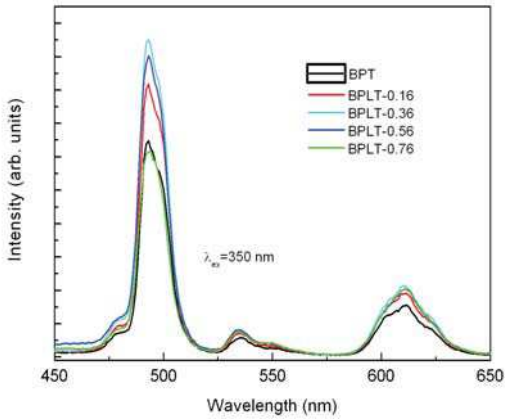

Fig. 9. Photoluminescence spectra of BPLT-x thin films. From Ref. [58] Zhou, H., et al., J. Am. Ceram. Soc., 93, 2109 (2010) Copyright American Ceramic Society (2010)

To understand the photoluminescence process in BPLT thin films excited under UV light, the excitation spectra by monitoring the emission at 493 nm and the transmission spectra of BPLT thin films were measured as shown in Fig.10 [58]. From Fig. 10 (a), it was observed that Pr doping or Pr-La codoping does not obviously influence the absorption spectra except the intensity of the broad band at around 350 nm. Meanwhile, the transmission spectra indicate that all the thin films with different La doping contents show a sharp absorption edge at around 350 nm as shown in Fig. 10 (b). The results showed that there is good agreement between excitation peak and absorption edge. This implies the possibility that the excitation energy from a UV light is first absorbed by the host lattice through the interband transition, and then the absorbed energy transfers from the host lattice to the activator Pr^{3+} ions.

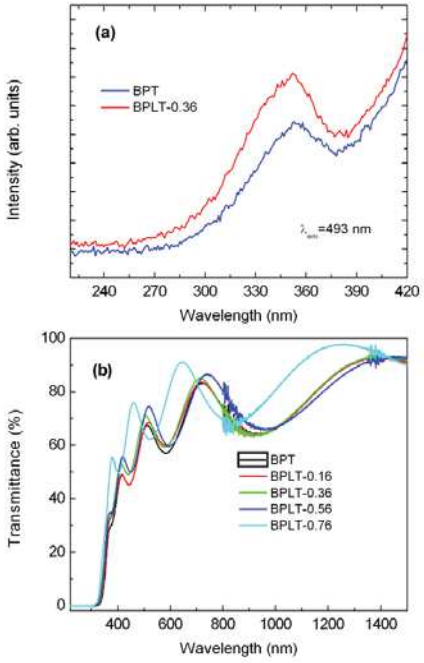

Fig. 10. Excitation and transmission spectra of BPLT-x thin films. From Ref. [58] Zhou, H., et al., J. Am. Ceram. Soc., 93, 2109 (2010) Copyright American Ceramic Society (2010)

The polarization-electric field (P-E) hysteresis loops of the BPLT-x thin films deposited on $Pt/TiO_2/SiO_2/Si$ substrates are measured. At an applied electric field of about 400 kV/cm, the remanent polarization (Pr) and coercive field (Ec) values of BPT and BPLT-0.36 films are 6.9 μC/cm², 147.3 kV/cm, and 19.8 μC/cm², 115.6 kV/cm, respectively. Obviously, the La^{3+} substitution raised Pr value of the BPT thin film from 6.9 to 19.8 μC/cm², and, at the same time, reduced the Ec value.

The polarization enhancement by La^{3+} substitution can be attributed to crystallization improvement of the thin films which has been confirmed by XRD and SEM. In addition, better crystallinity can also result in strong photoluminescence due to higher oscillating strengths for the optical transitions [41].

3.5 $(Bi, Er)_4Ti_3O_{12}$ luminescent ferroelectric thin films

As described before, BiT doped with Eu^{3+} or Pr^{3+} ions showed photoluminescence properties. However, they are only frequency down-conversion photoluminescence, up-conversion photoluminescence in BiT based thin films is also worth studying.

As is known, Er^{3+}/Yb^{3+} co-doped materials have been recognized as one of the most efficient systems for obtaining frequency up-conversion photoluminescence due to the efficient energy transfer from Yb^{3+} to Er^{3+} ions pumped by 980 nm [63,64], in which Er^{3+} ions acted as luminescence centers and Yb^{3+} ions as sensitizers. On the other hand, considering the lattice structure of BiT, Er^{3+}/Yb^{3+} ions can be accommodated in well defined sites of BiT lattice by substituting for Bi^{3+} ions without the need of charge compensation. Therefore, it is of much interest to study up-conversion luminescence properties of Er^{3+}/Yb^{3+} co-doped BiT thin films [65].

Figure 11 shows the up-conversion luminescence spectra for the BErT and BYET thin films under a 980 nm laser excitation at room temperature [65]. As can be seen from Fig.11, there are three distinct up-conversion emission bands, of which the two bands centered at 524 nm and 545 nm, correspond to strong green light emissions ascribed to $^2H_{11/2}$ to $^4I_{15/2}$ and $^4S_{3/2}$ to $^4I_{15/2}$ transitions of Er^{3+} ions, respectively, and another band centered at 667 nm to very weak red light emission originated from $^4F_{9/2}$ to $^4I_{15/2}$ transition of Er^{3+} ions. The green emission at 549 nm is 20 times as strong as the red emission at 667 nm. Meanwhile, BYET thin films exhibit higher green emission intensity by a factor of about 30 compared with BErT thin films. It is worth noting that the near pure green up conversion photoluminescence is bright enough to be clearly observed by the naked eyes. This indicates that the up-conversion photoluminescence efficiency of BiT thin films co-doped by Er^{3+} and Yb^{3+} has been greatly improved.

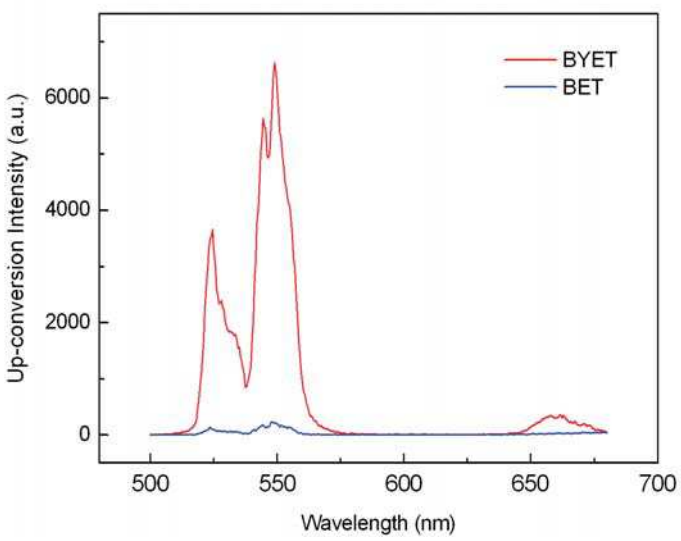

Fig. 11. Up-conversion luminescence spectra of BET and BYET thin films on fused silica substrates pumped by 980 nm. From Ref. [65] Gao, F., et al., J. Appl. Phys., 106, 126104 (2009). Copyright American Institute of Physics (2009)

4. Photoluminescence in other ferroelectric thin films

Reshmi, et al. studied photoluminescence of Eu^{3+}-doped $Ba_{0.7}Sr_{0.3}TiO_3$ thin films prepared by pulsed laser deposition [66]. The photoluminescence spectra show main transitions of Eu^{3+} ions at 550 nm ($^5D_1 \rightarrow ^7F_2$), 615 nm ($^5D_0 \rightarrow ^7F_2$), and 669 nm ($^5D_0 \rightarrow ^7F_3$) upon excitation with 408 nm. It was confirmed that the photoluminescence of BST:Eu thin films was closely correlated to the crystallinity.

Kuo, et al. studied photoluminescent properties of Er^{3+}-doped $Ba_{0.7}Sr_{0.3}TiO_3$ thin films prepared by sol-gel method [67]. The excitation-dependent PL studies indicate that the green emission peaks do not shift with the change in excitation power, while the integrated intensity increases monotonically with increasing excitation power.

Recently, Garcia Hernandez, et al. [68] also investigated photoluminescence of Er^{3+}-doped $BaTiO_3$ thin films prepared by sol-gel method. Their films exhibited green emissions under near-infrared excitation.

Aizawa and Ohtani studied the effect of Eu/Sr ratios on ferroelectric and fluorescent properties of Eu-substituted strontium bismuth tantalate (Eu-SBT) films grown on $Pt/Ti/SiO_2/Si$ substrates by spin-coating technique [69,70]. The remnant polarization values of the 260-nm-thick Eu-SBT films with Eu concentrations of 1.25 and 5 mol % were approximately 4.0 and 0.86 uC/cm^2, respectively. The PL intensity of the Eu-SBT films was significantly dependent on both annealing temperature and Eu concentrations. Emission peaks at approximately 600 nm were observed, which were associated with the $^5D_0 \rightarrow ^7F$ transitions of Eu^{3+}.

Nakajima, et al. prepared $Sr_{1-x}Pr_xTiO_3:Al^{3+}$ polycrystalline thin films using an excimer laser assisted metal-organic-deposition process at temperatures below 400 ^oC [71]. The Al^{3+}-added perovskite titanate thin films show strong red emission. The PL emission peaks were observed at 493, 533 and 612 nm, which are assigned to the transitions of $^3P_0 \rightarrow ^3H_4$, $^3P_0 \rightarrow ^3H_5$, $^1D_2 \rightarrow ^3H_4$ of Pr^{3+}, respectively. Host-to-activator energy transfer due to the coupling of the band-edge recombination energy and an allowed transition of a rare-earth ion is essential to provide a high efficiency of Al-doped $SrTiO_3:Pr^{3+}$ [72]. Nakajima, et al. also studied the substrate effect on excimer laser assisted crystal growth in $Ca_{0.997}Pr_{0.002}TiO_3$ polycrystalline thin films prepared by same method [73]. The thin films also show strong red luminescence. It was found that the substrate properties such as optical absorbance and thermal conductivity affected the crystal growth and the PL emission of the thin films in the excimer laser assisted metal organic deposition process.

Takashima, et al. observed intense red photoluminescence under ultraviolet excitation in epitaxial Pr-doped $Ca_{0.6}Sr_{0.4}TiO_3$ perovskite thin films prepared on $SrTiO_3$ (100) substrates by pulsed laser deposition [74]. The observed sharp PL peak centered at 610 nm was assigned to the transition of Pr^{3+} ions from the $^1D_2$ state to the $^3H_4$ state. It was suggested that the UV energy absorbed by the host lattice was transferred to the Pr ions, leading to the red luminescence.

Rho, et al. prepared $SrTiO_3$ thin films by rf-sputtering and studied the photoluminescence of the thin films after postannealing treatments [75]. The remarkable room temperature PL effects observed are contributed to both metastable and energetically stabilized defect states formed inside the band gap.

Moreira, et al. [76] studied photoluminescence of barium titanate and barium zirconate in multilayer disordered thin films at room temperature. The thin films were prepared by spin-coating and annealed at 350, 450, and 550 ^oC for 2 h. It was observed that the wide band

emission showed a synergic effect on barium zirconate and barium titanate thin layers in alternate multilayer system at room temperature by 488 nm excitation. Visible and intense photoluminescence was governed by $BaZrO_3$ thin films in the multilayer system. A disordered model was used to explained photoluminescence emission results of these multilayered systems.

Cavalcante, et al. [77] investigated the photoluminescent behavior of $Ba(Ti_{0.75}Zr_{0.25})O_3$ (BTZ) thin films experimentally and theoretically. The thin films were prepared by the polymeric precursor method. They suggested that the presence of localized electronic levels and a charge gradient in the band gap due to a symmetry breaking, be responsible for the PL in disordered BTZ lattice.

Ueda, et al. [78] studied photoluminescence from epitaxial perovskite-type alkaline-earth stannate thin films. The epitaxial calcium and strontium stannate films with perovskite or its related structure were fabricated by pulsed laser deposition method. The highly transparent films in the visible region showed intense luminescence of several colors under ultraviolet excitation.

5. Conclusion

Photoluminescence in low-dimensional oxide ferroelectric materials is of much interest. Lanthanide-doped $Bi_4Ti_3O_{12}$ thin films are promising photoluminescence ferroelectric materials. Co-doping of rare earth ions such as Eu/Gd, Pr/La, Er/Yb in bismuth titanate thin films is found to be an effective way to improve photoluminescence and electrical properties of the thin films. In addition, constructing nanocomposite thin films composed of ferroelectric $Bi_{3.6}Eu_{0.4}Ti_3O_{12}$ matrix and highly c-axis oriented ZnO nanorods can effectively enhance photoluminescent properties of Eu^{3+} ions. Our own studies suggest that rare earth doped $Bi_4Ti_3O_{12}$ thin films can be considered as a promising multifunctional material which can find applications in integrated multifunctional ferroelectric devices as well as in optoelectronic devices. Further research should be focused on understanding the physical mechanism of photoluminescence in low-dimensional oxide ferroelectric materials.

6. Acknowledgments

The author is grateful for the contributions from Drs. K.B. Ruan, H. Zhou, F. Gao, G. H. Wu, and X.M. Chen. The financial support from NSFC (Nos. 50872156 and U0634006), the Natural Science Foundation of Guangdong Province, China (Grant No. 10251027501000007), and the Specialized Research Fund for the Doctoral Program of Higher Education of China (Grant No. 20090171110007), is acknowledged.

7. References

[1] Warusawithana, M.P., Cen, C., Sleasman, C.R., Woicik, J.C., Li, Y.L., Kourkoutis, L.F., Klug, J.A., Li, H., Ryan, P., Wang, L.P., Bedzyk, M., Muller, D.A., Chen, L.Q., Levy, J., Schlom, D.G. (2009) *Science*, 324, 367-370.

[2] Paz de Araujo, C.A., Cuchiaro, J.D., McMillan, L.D., Scott, M.C., & Scott, J.F. (1995) *Nature (London)*, *374*, 627.

[3] Park, B.H., Kang, B.S., Bu, S.D., Noh, T.W., Lee, J., & Jo, W. (1999) *Nature (London)*, *401*, 682.

[4] Chon, U., Jang, H.M., Kim, M.G., & Chang, C.H. (2002) *Phys. Rev. Lett.*, *89,* 087601.
[5] Bao, D.H., Chiu, T.W., Wakiya, N., Shinozaki, K. & Mizutani, N. (2003) *J. Appl. Phys.*, *93*, 497.
[6] Bao, D.H., Lee, S.K., Zhu, X.H., Alexe, M. & Hesse, D. (2005) *Appl. Phys. Lett.*, *86,* 082906.
[7] Lee, H. N., Hesse, D., Zakharov, N. & Gösele, U. (2002) *Science*, *296*, 2006.
[8] Gu, B., Wang, Y.H., Peng, X.C., Ding, J.P., He, J.L. & Wang, H.T. (2004) *Appl. Phys. Lett., 85*, 3687.
[9] Hu, G. D., Fan, S. H. & Cheng, X. (2007) *J. Appl. Phys., 101,* 054111.
[10] Wang, Y. H., Gu, B., Xu, G. D. & Zhu, Y.Y. (2004) *Appl. Phys. Lett., 84*, 1686.
[11] Badr, Y., Salah, A., Battisha, I.K. (2005) *J. Sol-Gel Sci. & Technol.*, 34 (3): 219-226.
[12] Fu, Z., Moon, B.K., Yang, H.K., Jeong, J.H. (2008) *J. Phys. Chem. C*, 112 (15): 5724-5728 .
[13] Lemos, F.C.D., Melo, D.M.A., da Silva, J.E.C. (2005) *Mater. Res. Bull.*, 40 (1): 187-192.
[14] Lin, Y.H., Nan, C.W., Wang, J.F., He, H.C., Zhai, J.Y., Jiang, L. (2004) *Mater. Lett.*, 58 (5): 829-832.
[15] Oliveira, R. C., Cavalcante, L. S., Sczancoski, J. C., Aguiar, E. C., Espinosa, J. W. M., Varela, J. A., Pizani, P. S., Longo, E. (2009) *J. Alloys & Compds.*, 478 (1-2): 661-670.
[16] Pizani, P.S., Leite, E.R., Pontes, F.M., Paris, E.C., Rangel, J.H., Lee, E.J.H., Longo, E., Delega, P., Varela, J.A. (2000) *Appl. Phys. Lett.*, 77 (6): 824-826.
[17] Longo, V. M., Cavalcante, L. S., de Figueiredo, A. T., Santos, L. P. S., Longo, E., Varela, J. A., Sambrano, J. R., Paskocimas, C. A., De Vicente, F. S., Hernandes, A. C. (2007) *Appl. Phys. Lett.*, 90 (9): 091906.
[18] Motta, F. V., Marques, A. P. A., Espinosa, J. W. M., Pizani, P. S., Longo, E., Varela, J. A. (2010) *Curr. Appl. Phys.*, 10 : (1): 16-20.
[19] Cavalcante, L. S., Anicete-Santos, M., Sczancoski, J. C., Simoes, L. G. P., Santos, M. R. M. C., Varela, J. A., Pizani, P. S., Longo, E. (2008) *J. Phys. & Chem. Solids*, 69 (7): 1782-1789.
[20] Cavalcante, L. S., Simoes, A. Z., Espinosa, J. W. M., Santos, L. P. S., Longo, E., Varela, J. A., Pizani, P. S. (2008) *J. Alloys & Comp.*, 464 (1-2): 340-346.
[21] Ferri, E. A. V., Sczancoski, J. C., Cavalcante, L. S., Paris, E. C., Espinosa, J. W. M., de Figueiredo, A. T., Pizani, P. S., Mastelaro, V. R., Varela, J. A., Longo, E. (2009) *Mater. Chem. & Phys.*, 117 (1): 192-198.
[22] Gurgel, M. F. C., Espinosa, J. W. M., Campos, A. B., Rosa, I. L. V., Joya, M. R., Souza, A. G., Zaghete, M. A., Pizani, P. S., Leite, E. R., Varela, J. A., Longo, E. (2007) *J. Lumin.*, 126 (2): 771-778.
[23] de Figueiredo, A.T., Longo, V.M., de Lazaro, S., Mastelaro, V.R., De Vicente, F.S., Hernandes, A.C., Li, M.S., Varela, J.A., Longo, E. (2007) *J. Lumin.*, 126 (2): 403-407.
[24] Longo, V.M., Cavalcante, L.S., Costa, M.G.S., Moreira, M.L., de Figueiredo, A.T., Andres, J., Varela, J.A., Longo, E. (2009) *Theoretical Chemistry Accounts*, 124 (5-6): 385-394.
[25] Ma, Q., Zhou, Y.Y., Lu, M.K., Zhang, A.Y., Zhou, G.J. (2009) *Mater. Chem. & Phys.*, 116 (2-3): 315-318.
[26] Gu, H.S., Hu, Y.M., You, J., Hu, Z.L., Yuan, Y., Zhang, T.J. (2007) *J. Appl. Phys.*, 101 (2): 024319.
[27] Hu, Y.M., Gu, H.S., Sun, X.C., You, J., Wang, J. (2006) *Appl. Phys. Lett.*, 88 (19): 193120.
[28] Chen, G.Y., Qu,W.G., Ye, F., Zhang, W.X., Xu, A.W. (2008) *J. Phys. Chem. C*, 112 (43): 16818–16823.

[29] Yang, Y., Wang, X.H., Sun, C.K., Li, L.T. (2008) *J. Am. Ceram. Soc.*, 91, (11): 3820–3822.
[30] Liu L.F., Ning, T.Y., Ren, Y., Sun, Z.H., Wang, F.F., Zhou, W.Y., Xie, S.S., Song, L., Luo, S.D., Liu, D.F., Shen, J., Ma, W.J., Zhou, Y.L. (2008) *Mater. Sci. & Eng. B* 149: 41–46.
[31] Ida, S., Ogata, C., Unal, U., Izawa, K., Inoue, T., Altuntasoglu, O., Matsumoto, Y. (2007) *J. Am. Chem. Soc.*, 129 (29): 8956.
[32] Kang, B. S., Park, B. H., Bu, S. D., Kang, S. H. & Noh, T. W. (1999) *Appl. Phys. Lett., 75,* 2644.
[33] Lee, H. N. & Hesse, D. (2002) *Appl. Phys. Lett., 80*, 1040.
[34] Garg, A., Barber, Z. H., Dawber, M., Scott, J.F. & Barber, Z.H. (2003) *Appl. Phys. Lett., 83,* 2414.
[35] Lee, S.K., Hesse, D. & Gosele, U. (2006) *Appl. Phys. Lett., 88,* 062909.
[36] Ruan, K.B., Chen, X.M., Liang, T. Wu, G.H. & Bao, D.H. (2008) *J. Appl. Phys., 103,* 074101.
[37] Ruan, K.B., Chen, X.M., Liang, T. Wu, G.H. & Bao, D.H. (2008) *J. Appl. Phys., 103,* 086104.
[38] Pradhan, A. K., Zhang, K., Mohanty, S., Dadson, J. , Hunter, D., Loutts, G. B., Roy, U. N., Cui, Y., Burger, A. & Wilkerson, A. L. (2005) *J. Appl. Phys., 97,* 023513.
[39] Mercier, B., Dujardin, C., Ledoux, G., Louis, C., Tillement, O. & Perriat, P. (2004) *J. Appl. Phys., 96,* 650.
[40] Shim, K. S., Yang, H. K., Moon, B. K., Jeong, J. H., Yi, S. S. & Kim, K.H. (2007) *Appl. Phys. A, 88,* 623.
[41] Mishra, K. C., Berkowitz, J. K., Johnson, K. H. & Schmidt, P. C. (1992) *Phys. Rev., B 45,* 10902.
[42] Liu, Q.L., Bando, Y., Xu, F.F. & Tang, C.C. (2004) *Appl. Phys. Lett., 85*, 4890.
[43] Toda, K., Honma, T. & Sato, M. (1997) *J. Lumin., 71*, 71.
[44] Toda, K., Kameo, Y., Ohta, M. & Sato, M. (1995) *J. Alloys Comp., 218,* 228.
[45] Kim, K T., Kim, C. II., Kim, J. G. & Kim, G. H. (2007) *Thin Solid Films, 515*, 8082.
[46] Giridharan, N.V., Subramanian, M. & Jayavel, R. (2006) *Applied Physics, A83*, 123.
[47] Kim, S.S., Bae, J.C., & Kim, W.J. (2005) *J. Cryst. Growth, 274*, 394.
[48] Ruan, K.B., Gao, A.M., Deng, W. L. Chen, X.M. & Bao, D.H. (2008) *J. Appl. Phys., 104*, 036101.
[49] Bae, J.S., Shim, K.S., Kim, S.B., Jeong, J.H., Yi, S.S. & Park, J.C. (2004) *J. Cryst. Growth, 264*, 290.
[50] Zhou, H., Chen, X.M., Wu, G.H., Gao, F. Qin, N. & Bao, D.H. (2010) *J. Am. Chem. Soc.,* 132 (6):1790.
[51] Chong, M.K., Abiyasa, A.P., Pita, K. & Yu, S.F. (2008) *Appl. Phys. Lett., 93*, 151105.
[52] Shionoya, S. & Yen, W.H. (1998) Phosphor Handbook (CRC, Boca Raton, FL, USA), p.179.
[53] Jia, W., Monge, K. & Fernandez, F. (2003) *Opt. Mater., 23,* 27.
[54] Yu, Y. L., Wang, Y. S., Chen, D. Q., Huang, P., Ma, E. & Bao, F. (2008) *Nanotechnology, 19*, 055711.
[55] Du, Y.P., Zhang, Y.W., Sun L.D. & Yan, C.H. (2008) *J. Phys. Chem., C112*, 12234.
[56] Bang, J., Yang, H. & Holloway, P. H. (2005) *J. Chem. Phys., 123*, 084709.
[57] Tetsuka, H., Takashima, H., Ikegami, K., Nanjo, H., Ebina, T. & Mizukami, F. (2009) *Chem. Mater.*, *21*, 21.
[58] Zhou, H., Wu, G.H., Qin, N. & Bao, D.H. (2010) *J. Am. Ceram. Soc.*, 93, 2109.

[59] Takashima, H., Ueda, K. & Itoh, M. (2006) *Appl. Phys. Lett.*, *89,* 261915.
[60] Okamoto S. & Yamamoto, H. (2001) *Appl. Phys. Lett.*, *78*, 655.
[61] Goto, K., Nakachi, Y. & Ueda, K. (2008) *Thin Solid Films, 516*, 5885.
[62] Okumura, M., Tamatani, M., Albessard, A.K. & Matsuda, N. (1997) *Jpn. J. Appl. Phys, 36,* 6411.
[63] Wang, L. Y., Li, P. & Li, Y. D. (2007) *Adv. Mater., 19*, 3304.
[64] Lim, S. F., Riehn, R., Ryu, W. S., Khanarian, N., Tung, C. K., Tank, D. & Austin, R. H. (2006) *Nano Lett., 6*, 169.
[65] Gao, F., Wu, G.H., Zhou, H. & Bao, D.H. (2009) *J. Appl. Phys., 106*, 126104.
[66] Reshmi, R., Jayaraj, M. K., Jithesh, K., Sebastian, M. T. (2010) *J. Electrochem. Soc.*, 157 (7): H783-H786.
[67] Kuo, S.Y., Hsieh, W.F. (2005) *J. Vac. Sci. & Technol. A* , 23 (4): 768-772.
[68] Garcia Hernandez, M., Carrillo Romo, F. de J., Garcia Murillo, A., Jaramillo Vigueras, D., Meneses Nava, M. A., Bartolo Perez, P., Chadeyron, G. (2010) *J. Sol-Gel Sci. & Technol.*, 53 (2): 246-254.
[69] Aizawa, K., Ohtani, Y. (2007) *Jpn. J. Appl. Phys. Part 1*, 46 (10B): 6944-6947.
[70] Aizawa, K., Ohtani, Y. (2008) *Jpn. J. Appl. Phys. Part 2*, 47 (9): 7549-7552.
[71] Nakajima, T., Tsuchiya, T., Kumagai, T. (2008) *Curr. Appl. Phys.*, 8 (3-4): 404-407.
[72] Yamamoto, H., Okamoto, S., Kobayashi, H. (2002) *J. Lumin.*, 100 (1-4): 325-332.
[73] Nakajima, T., Tsuchiya, T., Kumagai, T. (2007) *Appl. Surf. Sci.*, 254 (4): 884-887.
[74] Takashima, H., Ueda, K., Itoh, M. (2006) *Appl. Phys. Lett.*, 89 (26): 261915.
[75] Rho, J., Jang, S., Ko, Y.D., Kang, S., Kim, D.W., Chung, J.S., Kim, M., Han, M., Choi, E. (2009) *Appl. Phys. Lett.*, 95 (24): 241906.
[76] Moreira, M. L., Gurgel, M. F. C., Mambrini, G. P., Leite, E. R., Pizani, P. S., Varela, J. A., Longo, E. (2008) *J. Phys. Chem. A*, 112 (38): 8938-8942 .
[77] Cavalcante, L. S., Gurgel, M. F. C., Paris, E. C., Simoes, A. Z., Joya, M. R., Varela, J. A., Pizani, P. S., Longo, E. (2007) *Acta Mater. A*, 55 (19): 6416-6426.
[78] Ueda, K., Maeda, T., Nakayashiki, K., Goto, K., Nakachi, Y., Takashima, H., Nomura, K., Kajihara, K., Hoson, H. (2008) *Appl. Phys. Exp.*, 1 (1): 015003 .

Ferroelectrics

Edited by Dr Indrani Coondoo

ISBN 978-953-307-439-9
Hard cover, 450 pages
Publisher InTech
Published online 14, December, 2010
Published in print edition December, 2010

Ferroelectric materials exhibit a wide spectrum of functional properties, including switchable polarization, piezoelectricity, high non-linear optical activity, pyroelectricity, and non-linear dielectric behaviour. These properties are crucial for application in electronic devices such as sensors, microactuators, infrared detectors, microwave phase filters and, non-volatile memories. This unique combination of properties of ferroelectric materials has attracted researchers and engineers for a long time. This book reviews a wide range of diverse topics related to the phenomenon of ferroelectricity (in the bulk as well as thin film form) and provides a forum for scientists, engineers, and students working in this field. The present book containing 24 chapters is a result of contributions of experts from international scientific community working in different aspects of ferroelectricity related to experimental and theoretical work aimed at the understanding of ferroelectricity and their utilization in devices. It provides an up-to-date insightful coverage to the recent advances in the synthesis, characterization, functional properties and potential device applications in specialized areas.

How to reference

In order to correctly reference this scholarly work, feel free to copy and paste the following:

Dinghua Bao (2010). Photoluminescence in Low-Dimensional Oxide Ferroelectric Materials, Ferroelectrics, Dr Indrani Coondoo (Ed.), ISBN: 978-953-307-439-9, InTech, Available from: http://www.intechopen.com/books/ferroelectrics/photoluminescence-in-low-dimensional-oxide-ferroelectric-materials

INTECH
open science | open minds

InTech Europe
University Campus STeP Ri
Slavka Krautzeka 83/A
51000 Rijeka, Croatia
Phone: +385 (51) 770 447
Fax: +385 (51) 686 166
www.intechopen.com

InTech China
Unit 405, Office Block, Hotel Equatorial Shanghai
No.65, Yan An Road (West), Shanghai, 200040, China
中国上海市延安西路65号上海国际贵都大饭店办公楼405单元
Phone: +86-21-62489820
Fax: +86-21-62489821